

# A Detailed Noise Characterization and Sensor Evaluation of the North Island of New Zealand Using the PQLX Data Quality Control System

by S. J. Rastin, C. P. Unsworth, K. R. Gledhill, and D. E. McNamara

**Abstract** In this paper we analyze five years of recordings (2005–2009) from the National Seismograph Network in the North Island of New Zealand using the power spectral density probability density function (PDF) method of [McNamara and Buland \(2004\)](#). At each station the ambient noise is characterized and the stable noise model is then represented with the modes of the corresponding PDFs over all periods. Obtaining such an accurate long-term noise baseline for each station provides a reference model that should serve to prioritize maintenance issues for the network operators. The PDF mode low-noise model (MLNM) for the North Island is then obtained from the minimum of all the noise modes at each period. The maximum and minimum differences between the North Island MLNM and the noise mode model periods are then calculated at each station as a quick assessment tool. The daily and seasonal variations of the noise mode model are then characterized, and the horizontal and vertical mode noise models are then compared at each station. The applied technique is practical for evaluating the cultural noise condition and the earthquake detection capability, as well as the installation design against unwanted tilt and temperature variation.

*Online Material:* Stable noise models from PDFs, and daily/seasonal model variations.

## Introduction

Developing efficient methodologies for seismic data processing over a network of seismographs requires assessing the performance of each seismograph as well as evaluating the ambient noise at each station. To assess the performance effectively, one should analyze the seismic recordings of each station collected over a long time. A seismographic recording includes earth vibrations as well as instrumentation noise. Earth vibrations can be either due to earthquakes or nonearthquake signals, where nonearthquake disturbances can originate from cultural or natural noise sources ([Havskov and Alguacil, 2004](#); [Wielandt, 2002](#); [Bormann, 2002](#)). At each seismographic station, the minimum and the maximum observable periods in the corresponding recordings are determined by the sampling rate and the installed sensor specification, respectively. For example, some broadband sensors can record the phenomena with a period content as long as 1000 s ([Havskov and Alguacil, 2004](#)). In addition, the noise level at each period depends on the noise sources in the station's neighborhood, as well as the installation quality of its sensors ([Webb, 2002](#)). All the aforementioned characteristics can be reflected by an appropriate noise model, which is an estimate

of the power spectral density (PSD) of the background ambient noise at the site.

To obtain the PSD that represents the noise baseline at each station, different nonparametric approaches have been taken. [Peterson \(1993\)](#) computed a new low-noise model (NLNM) and a new high-noise model (NHNM) by estimating the PSDs of the background noise at 75 stations in the Global Seismographic Network (GSN). To achieve this he applied averaging over the squared magnitude of the fast Fourier transform of the overlapping seismic data segments.

[McNamara and Buland \(2004\)](#) extended the [Peterson \(1993\)](#) noise estimation method by examining the distribution of PSDs using a PDF procedure. They computed a new noise model for the United States Geological Survey (USGS) Advanced National Seismic System based on the highest probability noise level rather than the low-noise floor of [Peterson \(1993\)](#).

Their PSD PDF procedure was then standardized in an open-source software package called PQLX (PASSCAL Quick Look eXtended) by Boaz ([McNamara and Boaz, 2006, 2011](#); [Boaz and McNamara, 2008](#)) for the Incorporated

Research Institutions for Seismology (IRIS). The PQLX software package is currently in operation at international organizations such as the USGS National Earthquake Information Center, IRIS Data Management Center, and recently GeoNet in New Zealand as a noise assessment tool (see [Data and Resources](#) section).

Recently, we applied PQLX to the recordings of the URZ station in the Bay of Plenty region of New Zealand. This confirmed that the computed noise models were accurate and consistent with the sensor installation and the available noise sources for a New Zealand station ([Rastin et al., 2010](#)).

In the work presented here, we apply this method to analyze five years of recordings (2005–2009) obtained from the National Seismograph Network in the North Island of New Zealand (see [Data and Resources](#) section). Our motivation was to produce a scheme that would serve as a useful and valuable reference source for future research work.

### The New Zealand National Seismograph Network

The New Zealand National Seismograph Network (NZNSN) consists of 46 broadband seismometers installed all over the North and South Islands ([Petersen et al., 2011](#)). The recordings of each station are continuously sent to the GeoNet data centers in Wellington and Taupo using high-speed data connections mainly based on a VSAT platform provided by Optus of Australia ([Gledhill, 2004](#)). The data are then automatically and manually processed to produce the New Zealand earthquake catalog and archived for ongoing research use (see [Data and Resources](#) section).

The mission of the NZNSN is to record and report on New Zealand earthquakes. GeoNet locates 15,000–20,000 earthquakes in an average year. All but two of the broadband sensors in the network are surface mounted with approximately 1-m-square vaults set as much as 1-m deep into the ground. The remaining two sites employ 50-m deep boreholes and borehole sensors. If surface rock exposures exist, the vaults are built into the rock; otherwise they are built into the most competent ground available. The vaults are insulated, but the sensors are not wrapped in material to prevent air circulation. The NZNSN stations are located around New Zealand with a spacing of approximately 100 km, with almost all located in rural areas with relatively low levels of cultural noise.

In this study 19 broadband seismometers from the NZNSN in the North Island are considered for the background noise analysis. The map of the National Seismograph Network on the North Island is shown in [Figure 1](#).

The list of the stations, their locations, and information on the geology at each site are given in [Table 1](#), along with the history and type of the corresponding sensors within the interval of interest are presented. Depending on the geographical location, sensor type, and installation the noise baseline differs from one site to another. Furthermore, the

noise energy at each period varies on the daily and seasonal bases that can affect the quality of recordings.

### Noise Model Estimation Method

Because a seismographic record is a stochastic signal, its corresponding PSD can be estimated by means of averaging. Detailed PSD calculation for a stochastic signal from a wide-sense-stationary process can be found in [Bendat and Piersol \(1986\)](#), [Oppenheim et al. \(1999\)](#), and [Stensby, 2011](#).

In order to obtain the PSD of the baseline noise at different stations, [Peterson \(1993\)](#) restricted the seismic recordings to the ones with no transient phenomena, such as noise bursts, earthquakes, and data gaps. This way the stationary assumption was kept valid for applying the corresponding math.

[McNamara and Buland \(2004\)](#) suggested a new statistical approach to automatically remove the nonstationary parts while using the same algorithm to estimate the PSDs. The method is based on calculating the PDF from the obtained PSDs of a large number of data sets. Therefore, all transients are discriminated as they are less likely to occur, and the power values with high probability of occurrence at each period represent the stationary background ambient noise at each station. This method is the basis of the PQLX software package that has been applied to this study ([Boaz and McNamara, 2008](#)). A full description of the PSD and PDF calculations from the data recorded at each station during the time interval of interest can be found in [McNamara and Buland \(2004\)](#). Converted to the ground acceleration, final PSD estimates are in units of decibels (dB) relative to  $1 \text{ (m}^2/\text{s}^4)/\text{Hz}$  and have a 95% level of confidence that the spectral point lies within  $-2.14$  to  $2.87$  dB of the estimate, based on the number of segments averaged ([McNamara and Buland, 2004](#)). [Figure 2](#) shows an example of the calculated PDFs for different periods obtained from the PSDs for each January for five years (2005–2009) for the URZ station.

In order to obtain a noise model for each station, the PSD PDF method was applied to the three-component data recordings of each station, and the noise PDFs from all available recordings during the time interval of interest (2005–2009) were obtained ([Fig. 3](#)). The high-probability region represents the power values corresponding to the stationary background noise. Lower probability high-power PSDs are generally due to transients such as spiking, data gaps, calibration pulses, and earthquakes.

### Results

#### Analysis of the Noise PDFs, Sensor Malfunction, and Recording System Transients

Earth vibrations due to earthquake and nonearthquake events affect the seismic recordings. In addition, the recordings can be contaminated by the electronic and mechanical instrumentation noise ([Bormann, 2002](#); [Wielandt, 2002](#)). Because all data are included, the PSD PDF is useful for seismic station quality control. For example, bimodal distribution



**Figure 1.** Map of the New Zealand National Seismic Network stations (black circles) in the North Island of New Zealand (from Geonet; see [Data and Resources](#) section).

of PSDs in the PDFs is generally due to long-term sensor malfunction and replacement. If sensor replacement was an issue, the noise models were compared before and after sensor replacement. The daily and seasonal variations of the noise models at each station were then studied. Finally in order to study the effect of temperature and unwanted tilt, the

horizontal and vertical noise models were compared at each station.

The effect of sensor failure was observed in the noise PDFs of the BFZ station. Furthermore, sensor replacements affected the noise PDFs of the KNZ and TOZ stations (see Table 1).

Table 1  
National Network Stations of the North Island: Location, Geology, and Sensor History\*

Station Code <sup>†</sup>	Latitude, Longitude (°)	Place	Geology: Bedrock, Strength <sup>‡</sup>	Last Sensor in Operation from (yyyy/mm)	Sensor Type: Manufacturer and Model <sup>§</sup>	Previous Sensor Start Date (yyyy/mm)	Sensor Type: Manufacturer and Model <sup>§</sup>
Ouz	-35.22, 173.59	Omahuta	Limestone, MS	2003/08	Str STS-2		
WCZ	-35.94, 174.34	Waipu Caves	Greywacke, MS	2009/10	Gur CMG-3ESP	2005/05 2005/07	Gur CMG-3ESP Gur CMG-3ESP
KUZ	-36.74, 175.72	Kuaotunu	Greywacke, S	2004/02	Gur CMG-3ESP		
HAZ <sup>  </sup>	-37.75, 177.78	Maungaroa Station, Te Kaha	Weathered/fractured greywacke	2010/01	Gur CMG-3ESP		
MXZ	-37.56, 178.30	Matakoia Point	Basalt, MS	2009/08	Gur CMG-3ESP	2004/02 2009/08	Gur CMG-3ESP Gur CMG-3ESP
PUZ	-38.07, 178.25	Puketiti	Sandstone, MS	2003/08	Gur CMG-3ESP		
URZ	-38.26, 177.11	Matahi Valley, Urewera	Greywacke, MS	2002/02	Gur CMG-3TB		
MWZ	-38.33, 177.52	Kiriroa, Matawai	Siltstone, MS	2004/02	Gur CMG-3ESP		
TOZ	-37.73, 175.50	Tahuroa Rd., Waikato	Siltstone, MS	2008/12	Gur CMG-3ESPC	1998/10	Gur CMG-40T-30S
KNZ	-39.02, 177.67	Kokohu	Siltstone	2009/04	Gur CMG-3ESPC	1998/10	Gur CMG-40T-30S
TLZ <sup>#</sup>	-38.32, 175.53	Tolley Rd., Te Awamutu	Ignimbrite	2009/05	Gur CMG-3ESP		
HIZ	-38.51, 174.85	Hauti	Siltstone, MS	2004/02	Str STS-2		
BKZ	-39.16, 176.49	Black Stump Farm	Greywacke, MS	2004/02	Str STS-2		
VRZ	-39.12, 174.75	Vera Rd., Whangamomona	Mudstone, MS	2005/02	Gur CMG-3ESP	2003/12	Gur CMG-3ESP
WAZ	-39.75, 174.98	Whanganui	Siltstone, W	2003/07	Gur CMG-3ESP		
TSZ	-40.06, 175.96	Takapari Rd., Manawatu	Greywacke, MS	2004/01	Gur CMG-3ESP		
PXZ	-40.03, 176.86	Pawanui	Greywacke, S	2005/08	Gur CMG-3ESP		
BFZ	-40.68, 176.24	Birch Farm, Wairarapa	Sandstone, MS	2007/11	Str STS-2	2003/07	Str STS-2
MRZ	-40.66, 175.57	Mangatainoka River, Wairarapa	Greywacke, MS	2003/07	Gur CMG-3ESP		
WEL**	-41.28, 174.76	Wellington, Dominion Observatory	Greywacke, W	2008/12	Gur CMG-3ESP		

\*See [Data and Resources](#) section.

<sup>†</sup>For all the stations the depth is zero, except for the URZ, which is 50 m.

<sup>‡</sup>Strength: MS, moderately strong; S, strong; and W, weak.

<sup>§</sup>Manufacturers: Str, Streckheisen; Gur, Güralp. (When sensors were replaced, each replacement is noted.)

<sup>||</sup>The HAZ station in Te Kaha has been recently opened (January 2010) and hence is out of the scope of this study.

<sup>#</sup>The Tolley Road station (TLZ) recordings have been studied since May 2009, when it began operation.

\*\*The Wellington station (WEL) was upgraded at the end of 2008 to join the New Zealand National Seismograph Network (NZNSN), and no broadband sensor was installed for this station between 1995 and 2008. Therefore only the recordings of 2009 were considered for this station.

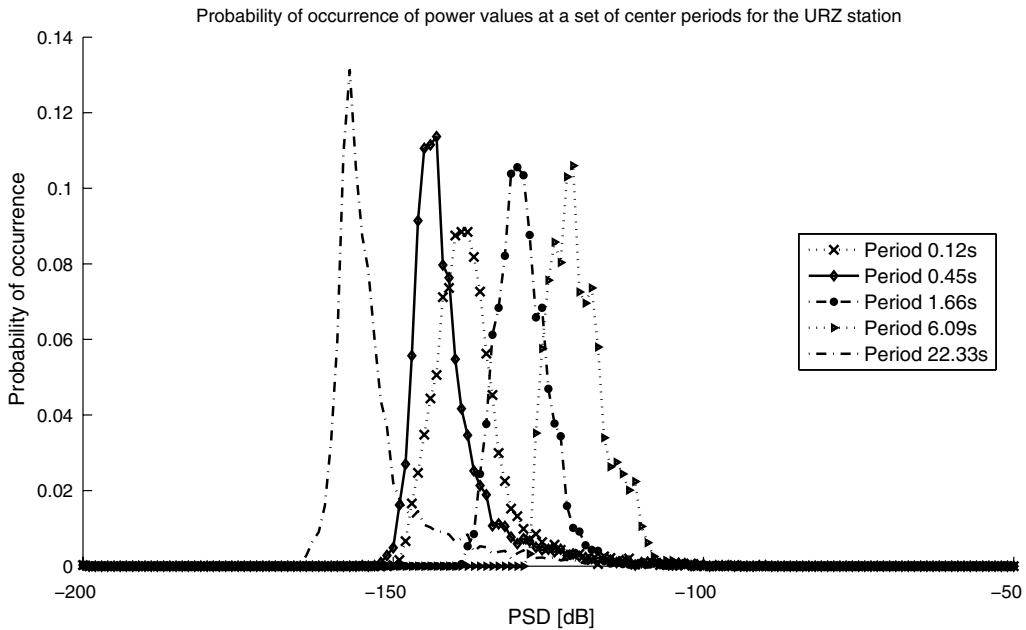


**Figure 2.** Probability of occurrence (y axis) of the power values (x axis) for the center periods 0.12, 0.45, 1.66, 6.09, and 22.33 s obtained for the URZ station from the PSDs for January for the five years from 2005 to 2009.

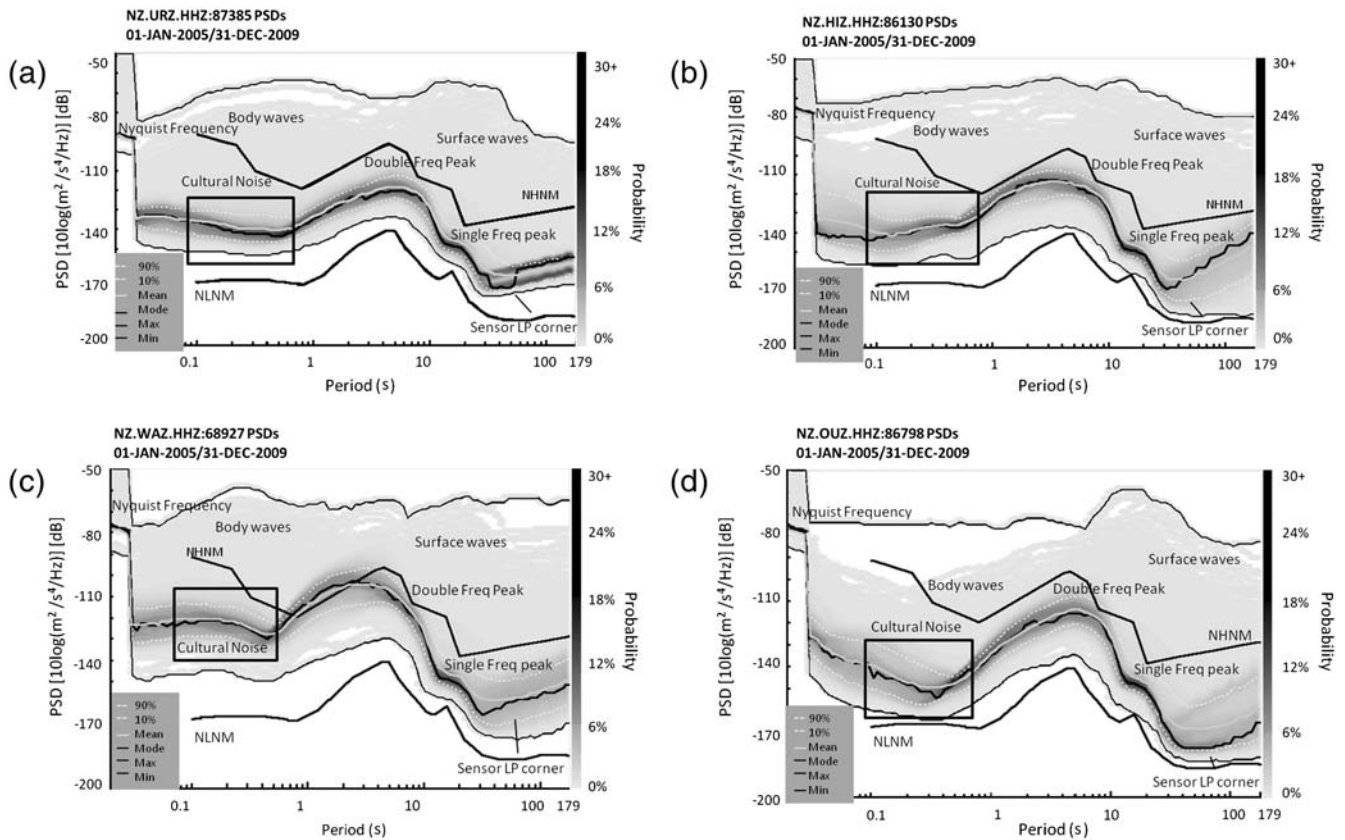


**Figure 3.** The noise PDFs obtained for stations (a) URZ, (b) HIZ, (c) WAZ, and (d) OUZ. Ambient noise sources are shown in their corresponding bands and probability of occurrence. The period band containing the cultural noise sources' energy is shown by a black rectangle in each plot. (LP, long period.)

In addition, to check the stability of the noise model, the occurrence of low-probability power values due to the system transients were studied in the PDFs of each station.

### Ambient Noise Sources

In this study the vibrations from the natural and cultural noise sources at the seismograph sites of the North Island are characterized. Furthermore, the effect of installation quality on the noise baseline is studied. The most common natural noise sources are wind, rain, rivers, oceanic microseisms, and earthquakes (Withers *et al.*, 1996; Webb, 2002; McNamara and Buland, 2004).

### Noise Characterization for the North Island National Broadband Seismographic Sites

*Stable Noise Models.* Applying the strategy explained previously in this paper, the noise PDFs for each station (with the exception of HAZ) in the map of Figure 1 were obtained and the stationary background noise was then characterized by the power values with the highest probability of occurrence over the whole time interval. The HAZ station in Te Kaha has not been included as it was only opened in January 2010 and hence is out of the scope of this study.

Examples of the obtained noise PDFs from five years of vertical recordings for four stations (URZ, OUZ, HIZ, and

WAZ) are presented in Figure 3. Each plot includes the minimum, maximum, mean, mode, 10th and 90th percentiles of the obtained PDFs. Also, the periods corresponding to the main ambient noise sources are specified in the obtained noise models. The single and double frequency peaks related to the oceanic microseism are recognizable in the plots of Figure 3, as expected (Hedlin and Orcutt, 1989; Webb, 2002; McNamara and Buland, 2004; Kurrle and Widmer-Schmidrig, 2010).

Low-probability (1–3%) high-power events in short and long periods can be attributed to body and surface waves generated by earthquakes. This is because they are not frequently observed in comparison to the microseisms and man-made noise (McNamara and Buland, 2004).

The period band containing the cultural noise sources' energy is shown by a black rectangle in each plot (periods < 1 s). The cultural noise levels differ from one site to another depending on the distance of the site from the farms, buildings, towns, roads, and industrial plants (Webb, 2002; Havskov and Alguacil, 2004; McNamara and Buland, 2004). The daily variation of the noise energy results in observing multibranches and lack of concentration in the high-probability values in the corresponding band. This case is illustrated in Figure 4 for the noise PDFs of the OUZ station. Two small areas were considered in the cultural noise band. One contains the larger power values with the high

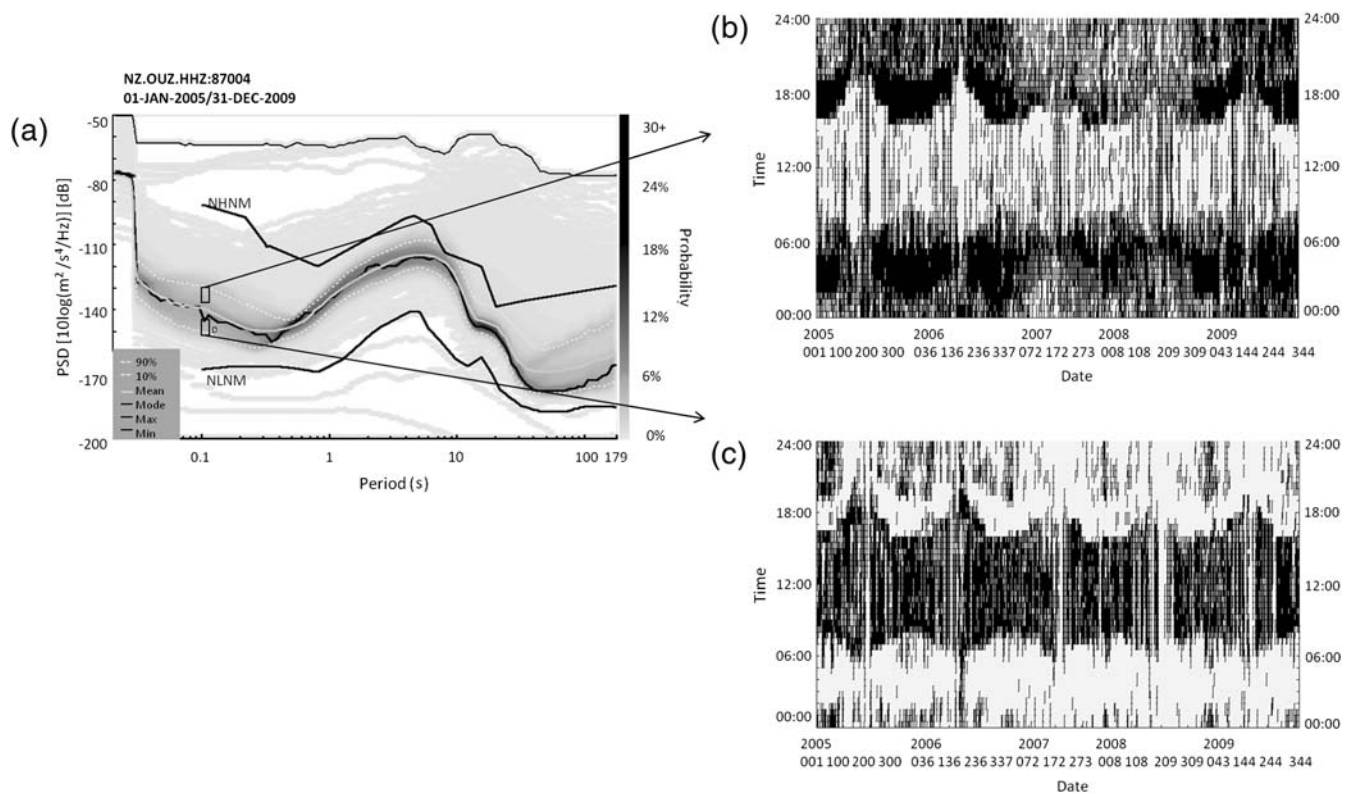


**Figure 4.** Diurnal variation of cultural noise energy for the OUZ station. (a) Noise PDFs obtained from five years of recordings: two black rectangles are considered in the cultural noise band. (b) PSD start times: the dates and times corresponding to each area are displayed, respectively. One-hour-long black lines mark the absolute time of the data records forming the PSDs of the selected area.

probability of occurrence and the other one covers the smaller power values. The corresponding dates and times for each area are displayed. The lower values correspond to data recorded within the overnight hours starting from 06:00 to 18:00 GMT (Greenwich Mean Time) or 6 p.m. to 6 a.m. New Zealand time. This makes sense because industrial units and offices are closed in this interval and hence the man-made noise energy should be at its minimum level. This pattern is repeated for all five years. In addition, every year the number of hours with less noise energy reaches a peak during winter (June–July). The daily and monthly variations of the obtained noise models for the selected stations are studied in a later section ([Daily and Seasonal Variations](#)).

Apart from the effect of the nearby noise sources, the quality of installation has a significant role in the level of the noise energy at each period ([Webb, 2002](#); [Wielandt, 2002](#)). For the stations with the surface vaults like the OUZ station (see [Table 1](#)), the quality of recordings is more affected by the surface modes propagating due to human activity compared to that of the stations with the borehole sensors. As can be seen in [Figure 3](#) for a deep-borehole installed sensor like that of the URZ station ([Table 1](#)), the power values of the highest probabilities in the cultural noise band are more concentrated and the variation is less compared to surface stations. Furthermore, the level of the PDF noise mode is relatively low as the borehole can filter a great amount of the cultural noise.

Moreover, the effect of the geology on the installation quality and therefore on the noise energy level should be taken into account ([Bormann, 2002](#); [Wielandt, 2002](#)). For example, for the WAZ station the power values with high probability between 0.7–2.6 s exceed the Peterson NHHM ([Peterson, 1993](#)). The high noise level in this band can be attributed to the geology of the area where the WAZ sensor

is installed. Kilometers of sediments in the Whanganui basin, where the WAZ station is located, amplify the microseisms.

Noise PDFs obtained from the vertical channels for the rest of the stations are presented in [Appendix S1](#), which is available as an electronic supplement to this paper. For the KNZ and TOZ stations, the noise PDFs were obtained from the recordings of the recent sensors (Gurlap CMG-3ESPC) because the range of the previous sensors did not cover periods as long as 60 s. For these stations, the noise characteristics were highly improved at both long and short periods after replacing the short-period sensors (CMG-40T-30S) with the broadband ones.

The obtained plots indicate that the ambient noise levels are higher than the Peterson NLNM ([Peterson, 1993](#)). All the obtained models are relatively stable as the gap between the 10th and 90th percentiles across the entire band remained small.

*Mode Noise Models.* We represented each stable noise model with the modes of the corresponding PDFs over all periods. The representative noise modes together with the Peterson NLNM and NHHM ([Peterson, 1993](#)) are shown in [Figure 5](#). Obtaining an accurate long-term noise baseline for each station helps to evaluate the cultural noise condition and the earthquake detection capability, as well as the installation quality at the corresponding site. In addition, it provides a reference that helps to detect the outliers/transients due to instrumentation problems for the network operators ([McNamara and Buland, 2004](#); [McNamara et al., 2009](#)).

We then obtained the PDF mode low-noise model (MLNM) ([McNamara and Buland, 2004](#)) from the minimum of all the modes at each period. The North Island MLNM lies above the Peterson NLNM ([Peterson, 1993](#)) over the whole period range. This was expected as the MLNM is the minimum

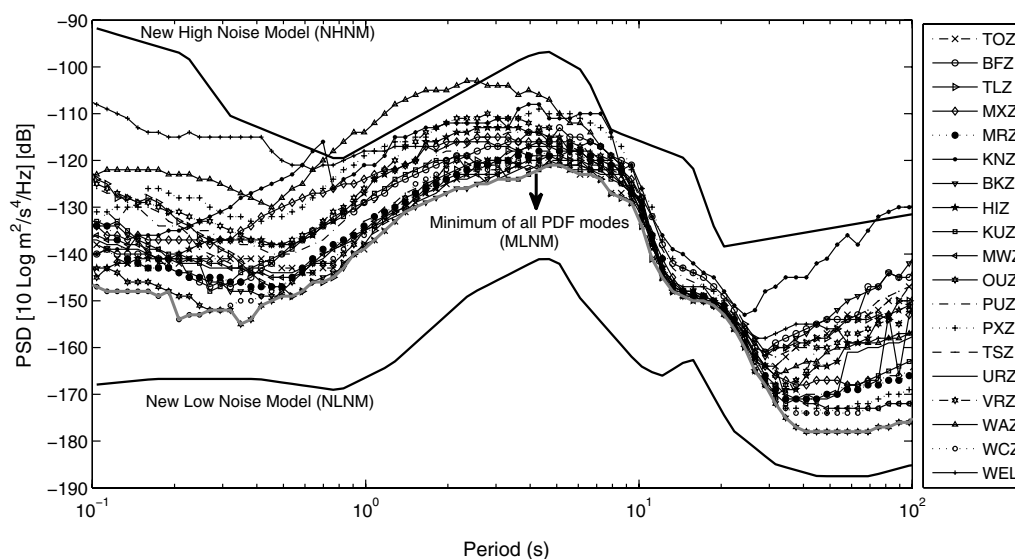


**Figure 5.** The mode noise models obtained from the noise PDFs of the North Island stations together with the Peterson NLNM and NHHM ([Peterson, 1993](#)). The PDF mode low-noise model (MLNM) was obtained for the North Island.

of the most commonly occurring noise levels in the North Island stations, while the Peterson NLNM was computed using only the quietest time periods at stations located deep inside continents and far from coastlines.

The difference between the North Island MLNM and the Peterson NLNM (Peterson, 1993) ranges from about 9 dB at longer periods (about 40 s) to 33 dB in the double frequency microseism band (9 s). Environmental properties of the island justify observing differences of about 30 dB between the obtained MLNM and the NLNM in the microseism band. In addition, for the period interval 0.1–0.9 s that covers the cultural noise band, the MLNM level is about 12–27 dB higher than that of the NLNM.

Comparing the mode noise models around the period 1.28 s showed that, for the stations located near coastlines, the noise levels are 38–55 dB higher than that of the NLNM. However, these differences range from 28 to 34 dB at the TOZ, TLZ, MRZ, BKZ, MWZ, OUZ, TSZ, URZ, and WCZ stations with more distance from the coastlines (see Fig. 1). The greater values and larger range of differences for the coastal sites can be attributed to the energy of coastal short-period ocean wave activity.

In the period band of the primary microseism (10–16 s), a small variation of 8 dB was observed across the network. This small variation suggests a similar source region. The largest primary microseism levels were obtained at stations KNZ and PXZ (–126 dB), which are located in the eastern coastal area of the Hawks Bay region. The lowest level was observed at the Tolley road station (TLZ) at the south of Te Awamutu (–134 dB), which is located far from the coastlines (see Fig. 1).

The variation of the secondary microseism peak was about 15 dB. While the largest double frequency peak was

observed at the WAZ station (–106 dB), the next largest peaks at this period were again observed at coastal stations KNZ and PXZ (–108 and –109 dB, respectively). As mentioned previously, the sedimentary bedrock in the Wanganui basin (near the WAZ site) has been found to magnify the microseisms.

For each station, the maximum and the minimum differences between the North Island MLNM and the noise PDF mode between 0.1 and 63.1 s are obtained and given in Table 2. The difference levels and their corresponding periods can provide a quick assessment tool. A minimal difference between PDF modes and the MLNM would show the periods in which stations perform well. In general, short-period noise depends on the proximity to cultural noise sources, while the noise of longer periods reflects the vault construction and insulation.

For example, the difference between the WEL noise PDF mode and the MLNM has reached its maximum value (40 dB) at 0.34 s. This implies that the WEL site either is noisy or the sensor isolation cannot filter the cultural noise (or a combination of both). For the WEL station the minimum difference (1 dB) was obtained at 18.8 s; therefore, cultural noise sources at this station have a larger impact on the station performance.

#### Daily and Seasonal Variations

*Daily Changes of the Mode Noise Model.* In order to evaluate the changes of the noise model during daytime hours in the different bands, we obtained the hourly variation of the noise PDF mode for each station (McNamara and Buland, 2004). We binned the PSDs for each hour from 00:00 GMT to 23:00 GMT within the time interval given in Table 2

Table 2  
The Maximum Difference between the Noise PDF Mode and the North Island MLNM in Periods 0.1–63.1 s

Station Name	Time Interval of the Obtained Stable Noise Model	Period Corresponding to the Maximum Difference* (s)	Maximum Difference* (dB)	Period Corresponding to the Minimum Difference (s)	Minimum Difference* (dB)
TOZ	12/2008 to 12/2009	57.92	25	0.91	0
BFZ	2005–2009	63.16	25	18.8	4
TLZ	5/2009 to 12/2009	57.92	24	0.54	0
MXZ	2005–2009	0.34	20	17.22	0
MRZ	2005–2009	0.11	14	18.8	0
KNZ	5/2009 to 12/2009	57.92	42	20.48	5
BKZ	2005–2009	63.16	29	0.49	0
HIZ	2005–2009	57.92	19	13.28	0
KUZ	2005–2009	0.12	15	3.32	0
MWZ	2005–2009	0.20	13	4.7	0
OUZ	2005–2009	7.89	8	0.19	0
PUZ	2005–2009	0.20	20	17.22	3
PXZ	2006–2009	0.20	26	28.96	1
TSZ	2005–2009	63.16	25	9.39	1
URZ	2005–2009	57.92	17	1.4	0
VRZ	2005–2009	0.20	23	14.48	0
WAZ	2005–2009	0.20	31	13.28	0
WCZ	2005–2009	2.15	6	0.10	0
WEL	2009	0.34	40	18.8	1

\*Difference between the noise PDF mode and the MLNM.

for each station. We then calculated the PDFs after obtaining the histogram at each period for each hour. We computed the noise model with its mode for each period. However, in some cases we obtained a PDF with two modes; that is, two power values with the identical chance of occurrence for that period. In such cases the PDF mode corresponding to the larger value was considered. Using the noise median would provide a smoother model. However, we wanted to study the daily variation of the largest and most probable noise power at each period. The daily variation of the mode noise for the URZ station is shown in Figure 6 as an example. The 3D plot shows the changes of the power values of the mode noise model (shaded bar) over the periods from 0.1 to 100 s (y axis) and the daily hour numbers (1–24) that span 00:00 GMT to 23:00 GMT ( $x$  axis). The mode noise daily variations for the other stations were obtained and given in (E) Appendix S2, which is available as an electronic supplement to this paper. It was found that in the periods shorter than 1 s, the noise baseline profile changes throughout the day. In general the cultural noise energy over the periods from 0.1 to 1 s increases from morning to the evening (7 a.m.–8 p.m. New Zealand local time). However, the silent interval differs in length and shifts slightly from one station to another, depending on the site location.

In order to evaluate each station's performance at the cultural noise band, the maximum value of the noise mode and its corresponding period (P1) were obtained and compared with the minimum value at the same period as shown in Figure 6. On the other hand, the minimum mode noise value and its corresponding period (P2) were obtained and compared with the maximum value at the same period. The two values obtained for the differences represent the maximum possible variations of the noise energy that can be observed over the P1–P2 period interval. The results are presented in Table 3.

For the PUZ, KUZ, WEL, and TLZ stations the value of the maximum possible noise variation is consistently high from P1 to P2. For these stations, the maximum possible variation reaches its largest value at period 0.104 s (18, 17, 15, and 15 dB respectively) and it only decreases 2–3 dB by the period P2. The recordings of these stations are affected the most by cultural noise. This can be either due to their location or the installation quality.

In contrast to these stations, the MXZ station has the lowest values of the daily variations over the P1 to P2 interval. The maximum amount of daily change for this station is 7 dB at 0.16 s. The maximum rate drops to 5 dB as it is extended to 0.27 s. Considering the fact the short-period noise did not show a large daily variation at the MXZ station, one can conclude that the energy due to local wave action can be the dominant source at periods shorter than 1 s for this station. It is consistent with the location of the MXZ (at Matakaoa Point; see Fig. 1). The maximum difference between the mode noise at MXZ and the North Island MLNM was 20 dB at 0.34 s (see Table 2).

For some stations the amount of maximum possible variation is higher at period P1, and it dramatically falls down at period P2. An example of this type is the URZ station (see Fig. 6). The maximum variation at 0.104 s is 11 dB. However, this value goes down to 6 dB at 0.38 s. This can be attributed to the deep-borehole installation of the URZ sensor. In fact, it can be inferred that the borehole has filtered the noise energy in periods longer than 0.175 s.

For longer periods up to 30 s, the noise character generally did not show strong diurnal dependency. The daily changes of the noise for longer periods can be due to the temperature effects. This is studied in a later section ([Temperature and Tilt Effects](#)).

*Seasonal Variations of the Mode Noise Model.* In addition to studying diurnal changes of the noise model, the seasonal

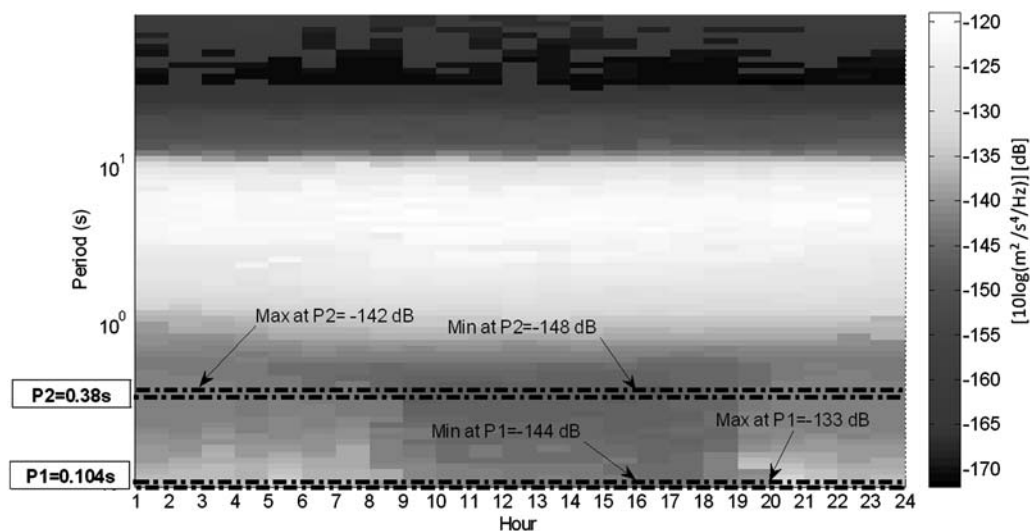


**Figure 6.** The diurnal variations of the vertical mode noise models obtained from the hourly data recorded over five years (January 2005–December 2009) for the URZ station.

Table 3  
The Maximum Daily Variations of the Noise Energy in the Cultural Noise Band for Each Station

Station Name	Maximum Value	P1: Corresponding Period (s)	Minimum Value at P1	Difference (dB)	Minimum Value	P2: Corresponding Period (s)	Maximum Value at P2	Difference (dB)
TOZ	-135	0.104	-148	13	-150	0.135	-139	11
BFZ	-132	0.104	-141	9	-151	0.247	-140	11
TLZ	-121	0.104	-136	15	-152	0.415	-139	13
MXZ	-132	0.160	-139	7	-140	0.27	-135	5
MRZ	-131	0.104	-145	14	-151	0.32	-144	7
KNZ	-131	0.208	-142	11	-144	0.113	-137	7
BKZ	-130	0.104	-145	15	-153	0.27	-143	10
HIZ	-136	0.247	-145	9	-151	0.104	-137	14
KUZ	-132	0.104	-149	17	-152	0.21	-138	14
MWZ	-135	0.104	-147	12	-150	0.27	-139	11
OUZ	-134	0.104	-152	18	-158	0.21	-148	10
PUZ	-125	0.104	-143	18	-144	0.16	-129	15
PXZ	-122	0.174	-137	15	-138	0.27	-126	12
TSZ	-120	0.104	-134	14	-148	0.349	-140	8
URZ	-133	0.104	-144	11	-148	0.38	-142	6
VRZ	-116	0.174	-137	21	-142	0.320	-135	7
WAZ	-117	0.104	-129	12	-134	0.349	-125	9
WCZ	-142	0.104	-154	12	-156	0.135	-144	12
WEL	-107	0.104	-122	15	-129	0.21	-115	14

variations were studied for each individual station. The PSDs for each month were retrieved for the time interval that gave a stable noise model for each station as shown in Table 2. The related PDF at each period was then estimated and the noise model was represented with its PDF mode for each month. In case of obtaining a PDF with two modes, the same strategy described in the previous section was taken.

Changes of the vertical mode noise models during the months of the year for the stations of interest were obtained and presented in Appendix S3, which is available as an electronic supplement to this paper. The TLZ and KNZ stations were excluded from this study as there were not enough recordings available to study the mode noise seasonal varia-

tions. (We require at least one year within the considered time interval of 2005–2009.) The KNZ new sensor and the Tolly Road station (TLZ) have been in operation since May 2009. The data recorded by the previous KNZ sensor were not suitable for studying the noise at periods longer than 12 s. As an example, the monthly variation of the mode noise for the VRZ station is shown in Figure 7. The plot shows the changes of the power values of the mode noise model (shaded bar) over the periods from 0.1 to 100 s (y axis) and the months of the year (x axis).

Study of the variations of the noise PDF modes during the months of the year showed that for some stations (TSZ, TOZ, VRZ, URZ, WAZ, WEL, and HIZ) the cultural noise

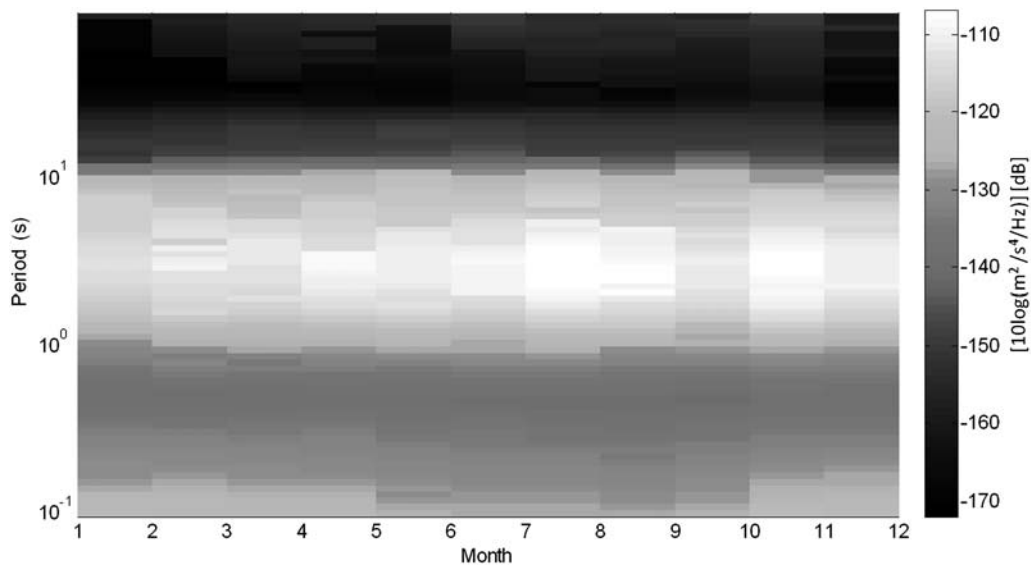


Figure 7. The monthly variations of the vertical mode noise model recorded over five years (January 2005–December 2009) at the VRZ station.

energy level increased from October to May (New Zealand spring–summer).

In addition, the peak value in the 1–4-s interval changes for different seasons. For 70.5% of the stations, the peak value in this period interval occurred in month 6 of the year, and for 17.5% of the stations the peak was equally observed during months 7 and 8. This is during the winter and can be due to the increase in ocean wave height related to more intense and frequent sea storms in the southern hemisphere winter (Bromirski and Duennebier, 2002; Aster *et al.*, 2008; Aster *et al.*, 2010). Monthly changes of the noise peak value in the aforementioned band for the OUZ, WCZ, MWZ, and KUZ stations are shown in Figure 8. Apart from the MWZ station with the maximum peak value at the month 8, for the other stations the maximum value was observed at the month 6. In addition, the peak value reached its minimum within the New Zealand warmer months. The decrease of the peak value in warmer seasons was smaller for the MWZ station (6 dB) compared to those of the OUZ, WCZ, and KUZ stations (10 dB).

In addition to the seasonal changes of the peak value in the 1–4-s interval, the noise peak level in the secondary microseism band (from 4 to 10 s) was found to show a seasonal change at different stations. The seasonal changes in the secondary microseism band were not only observed in the magnitude but were also seen in the periods corresponding to the noise peak levels. For the MWZ, URZ, MXZ, and BKZ stations the secondary microseism peak was shifted to the shorter periods during the southern hemisphere colder

months. The variation of the secondary microseism peak value and its corresponding period during the months of the year for the MWZ station are displayed in Figure 9. The maximum amplitude was observed in June; however, the corresponding periods continuously decreased from April to June and remained low until October. Microseism power is increased and enriched in short-period energy in the southern hemisphere winter.

### Temperature and Tilt Effects

Long-period seismometers are very sensitive to temperature variations. Therefore, appropriate shielding is required to protect them against temperature fluctuations (Bormann *et al.*, 1997). The lowest horizontal noise levels are observed at GSN stations where the sensors were installed in deep boreholes, tunnels, or very well-insulated vaults (Berger *et al.*, 2004). Furthermore, experimental results at the USGS Albuquerque Seismological Laboratory (ASL) have shown that a shallow borehole installation can cause a great reduction in the long-period horizontal noise level (Wilson *et al.*, 2002).

Here for a small group of the stations, a daily variation in the noise PDF mode was observed for periods longer than 35 s. The noise power level for stations KUZ, OUZ, and PUZ in this band showed an increase from late night to morning hours. These are all relatively close to the sea and have similar installation designs. This phenomenon has been illustrated for the OUZ station in Figure 10.

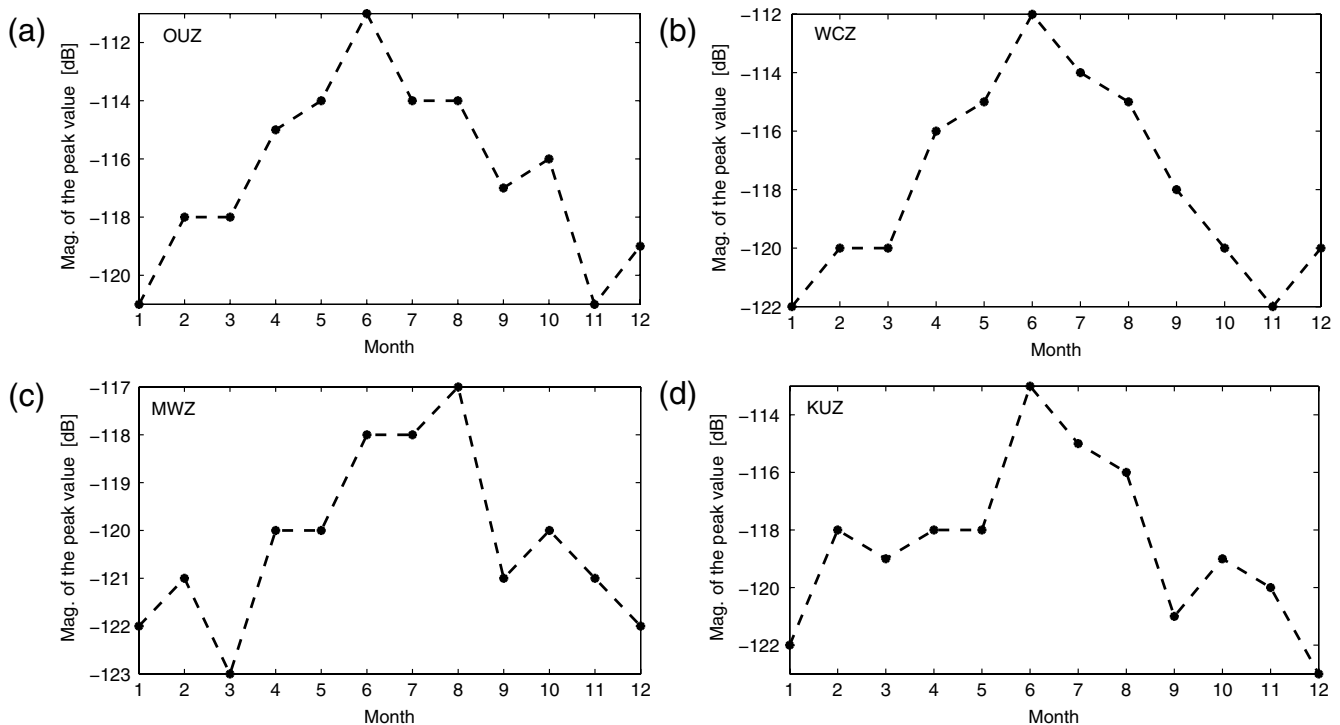


**Figure 8.** The monthly changes of the noise peak value in the short-period microseism band (1–4 s) for the stations (a) OUZ, (b) WCZ, (c) MWZ, and (d) KUZ.

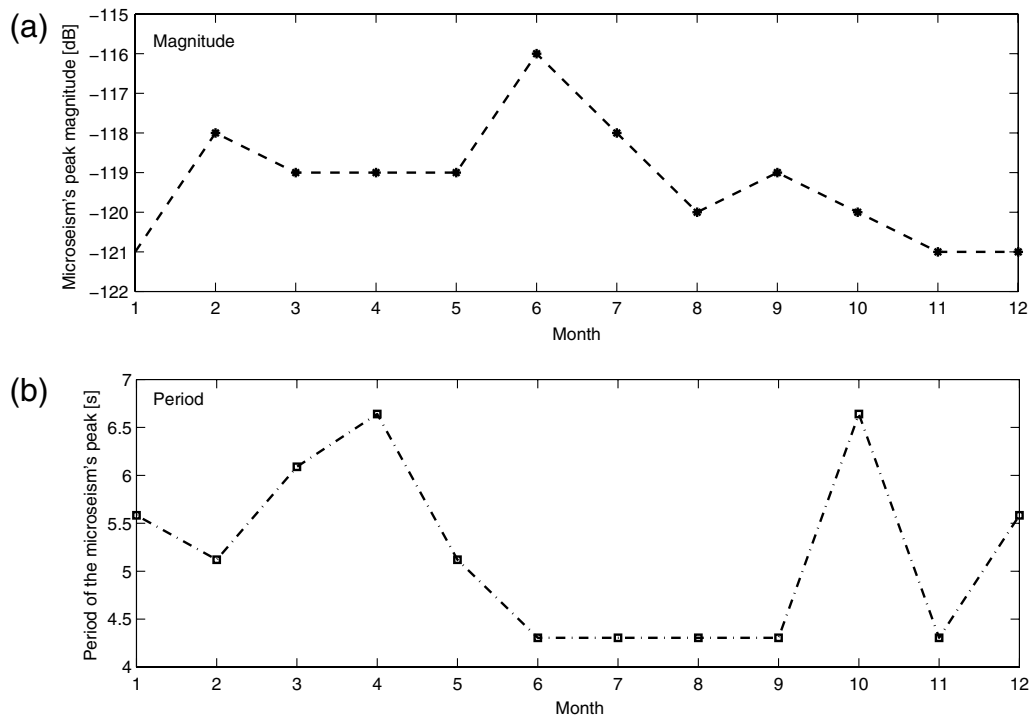


**Figure 9.** Monthly variation of (a) the secondary microseism peak value and (b) the corresponding period for the MWZ station.

Figure 10a shows the noise PDFs obtained for the OUZ station recordings of for 2005–2009. As can be seen, the high-probability area for the periods longer than 35 s has been split into two branches. The dates and times corresponding to the upper and lower branches (shown by two open black rectangles) are extracted and shown in Figure 10b,c. Furthermore, the daily and seasonal changes in the OUZ mode noise levels are given in Figures 10d and 10e, respectively. The effect of the split in the noise PDFs (Fig. 10a) has been reflected in the daily variation plot (Fig. 10d). The part corresponding to the upper branch is shown within the gray rectangle in the daily variation plot of Figure 10c.

The envelopes of the histograms (specified with gray ovals in Fig. 10b,c) have a periodic pattern during the years of study. The corresponding effect in the seasonal variation plot (Fig. 10e) can be seen inside the gray rectangle where the noise mode level reached its maximum levels from May to July.

The times and dates corresponding to this phenomenon show it mainly happened when the temperature was expected to be low. Therefore, the observed noise variation can be due to the vault construction and/or insulation issues.

The OUZ station is in a sheltered site by the side of a farm track, and hence the variation is less related to sun hit and the vault construction. Therefore, one hypothesis is that the noise is due to convection induced by the seismometer in the open space inside the insulation as it generates heat when it operates. This phenomenon has been observed by Holcomb *et al.* (1998) and suggests that an evaluation of insulation quality and vault design is recommended for this station.

KUZ is in an old gold mine and hence the temperature variation is likely to be small. In this case, we cannot make a definitive statement.

Variable surface loads, wind action on nearby structures, and fluctuations in the atmospheric pressure can produce unwanted tilt. The corresponding force will then affect the seismic mass in a similar way that the ground acceleration does (Wielandt, 2002). Horizontal components are always more sensitive to the tilt as the associated acceleration with gravity is rotated into them (Peterson and Orsini, 1976). In surface vaults, the long-period noise level in a horizontal component is usually 10–30 dB higher than that of the vertical component (Webb, 2002). For the surface vault instruments, we compared the horizontal (east–west component) and vertical mode noise models. The differences are plotted over the periods for the surface vault stations of the North Island in Figure 11. Averaging over the period interval 24–100 s showed that the maximum differences are observed in the VRZ (33.4 dB) and KUZ (32.1 dB) stations, and the minimum differences belong to stations KNZ and BKZ (13 dB and 14.7 dB, respectively). The averaged differences over periods 24–100 s, from the largest to the smallest, are given in Table 4.

The VRZ station is on mudstone and experiences tilt and long-period noise, particularly when the mudstone is water saturated in the winter. In this case the insulation will not improve the performance, and the unwanted tilt is unavoidable if a station is required in the area because the whole region has similar geology. An evaluation of insulation for the rest of the stations with the maximum differences

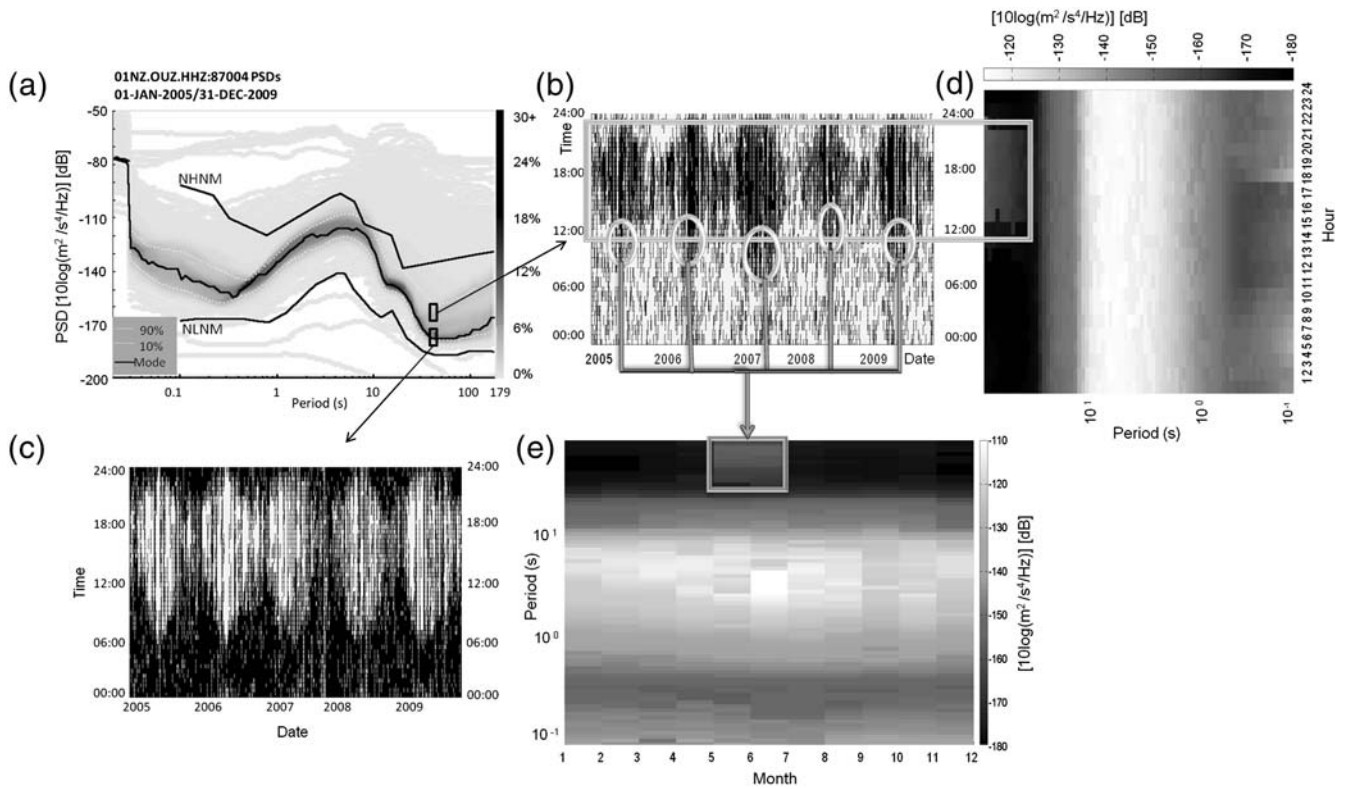


**Figure 10.** The variation of the long-period noise power (period > 35 s) for the OUZ station. (a) The noise PDFs obtained for the OUZ station from recordings made from 2005 to 2009: a split occurred in the power values with high probability of occurrence at period 35 s. The dates and times of the recordings (PSD start times) correspond to (b) the upper branch of the split and (c) the lower branch of the split. (d) The daily variations of the noise PDF mode: the effect of the split in the noise PDFs can be seen as hours with higher level of long-period noise (12–9 a.m New Zealand local time), as specified within the gray rectangle. These PDFs modes correspond to the recordings of the upper branch of the split. (e) Seasonal variations of the noise PDF mode: The effect of the periodic pattern in the envelope of the histogram (b); specified with gray ovals) can be seen inside the gray rectangle in (e), where the noise mode level has increased to its maximum levels from May to July.

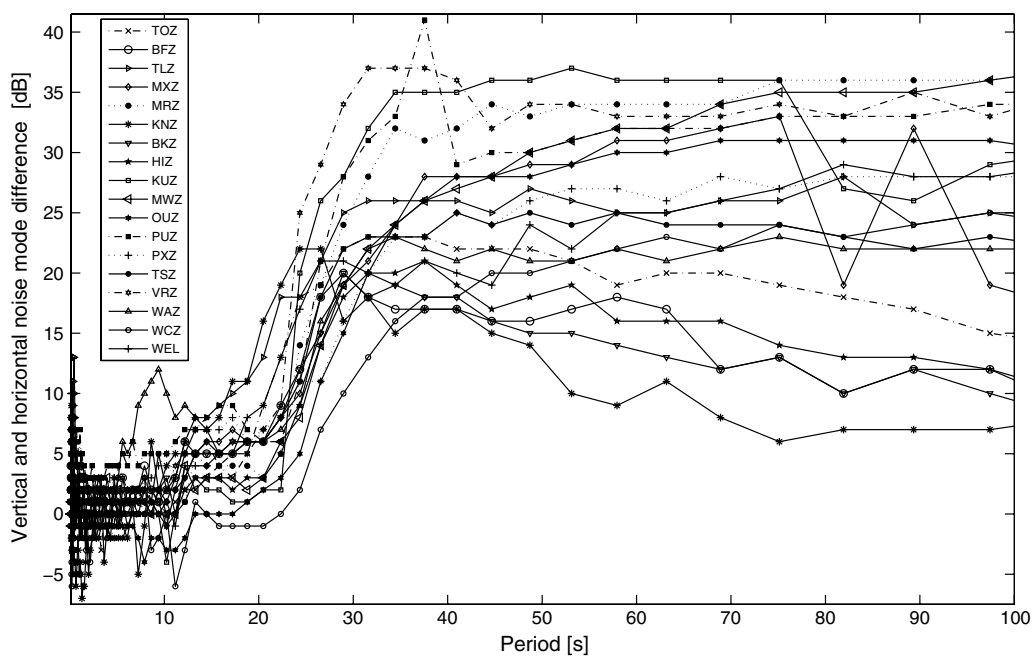


**Figure 11.** Difference between the vertical and horizontal mode noise models for the surface installed sensors in the North Island of New Zealand (see Table 4)

Table 4

Averaged Differences over Periods 24–100 s between the Horizontal and Vertical Mode Noise Models for the Surface Vault Instruments in the North Island

Station	Averaged Horizontal and Vertical Noise Difference (dB)
VRZ	33.4
KUZ	32.1
MRZ	31
PUZ	30.2
MWZ	27.5
OUZ	25.2
MXZ	25.1
TLZ	25
PXZ	23.4
WEL	23
TSZ	22.5
WAZ	20.5
TOZ	20.1
WCZ	18.1
HIZ	16.1
BFZ	15.4
BKZ	14.7
KNZ	13

is recommended. In particular, for the stations like KUZ with long-period noise variation, it should serve to improve the performance.

It has been shown that the deep-borehole installation can reduce the effect of atmospheric pressure up to 90% (Murphy and Savino, 1975). However, even with the borehole installation, the noise level in the horizontal component for periods longer than 20 s can be still higher than that of the vertical component and vary based on the installation quality. At ASL, this noise was attributed to the action of the air moving within the borehole around the sensor. They installed the sensor in sand at the bottom of the borehole in order to prevent

the air draft in the available volume, and they showed that it effectively reduced the difference between horizontal and vertical long-period noise (Holcomb *et al.*, 1998).

In our study, a Guralp CMG-3TB (Table 1) had been installed in a deep borehole for the URZ station. We studied vertical and horizontal noise PDFs obtained from the URZ recordings for five years. As can be seen in Figure 3a, there is a split in the noise PDFs plots. A similar split was observed in the horizontal noise PDFs. The corresponding dates of the split branches confirmed that it occurred in April 2007. Therefore, we obtained the vertical and horizontal noise PDF modes before and after the occurrence of the split using the recordings of the time intervals (2005–2006) and (2008–2009), respectively. The results are shown in Figure 12. For the time interval 2005–2006 and for periods longer than 20 s, the difference between horizontal and vertical mode noise is about 25 dB. However, this difference has reduced to –1 dB in the 20–50-s interval for the data recordings of 2008–2009. Because in practice the horizontal noise level is found to be greater than that of the vertical, this is an unusual observation. Over the entire time, the instrument response has not been updated, but the change may have been caused by a specific maintenance action taken around that date, possibly a centering of the sensor masses. Mass centering is known to be a problem at this station, although this should not cause a change in sensor response. What is clear is that, with a good borehole installation, the long-period horizontal and vertical noise levels should be similar.

### Conclusion

In this paper we analyzed recordings collected over five years (2005–2009) from the North Island stations of the New Zealand National Seismograph Network in order to characterize the noise and evaluate the performance for each site. To

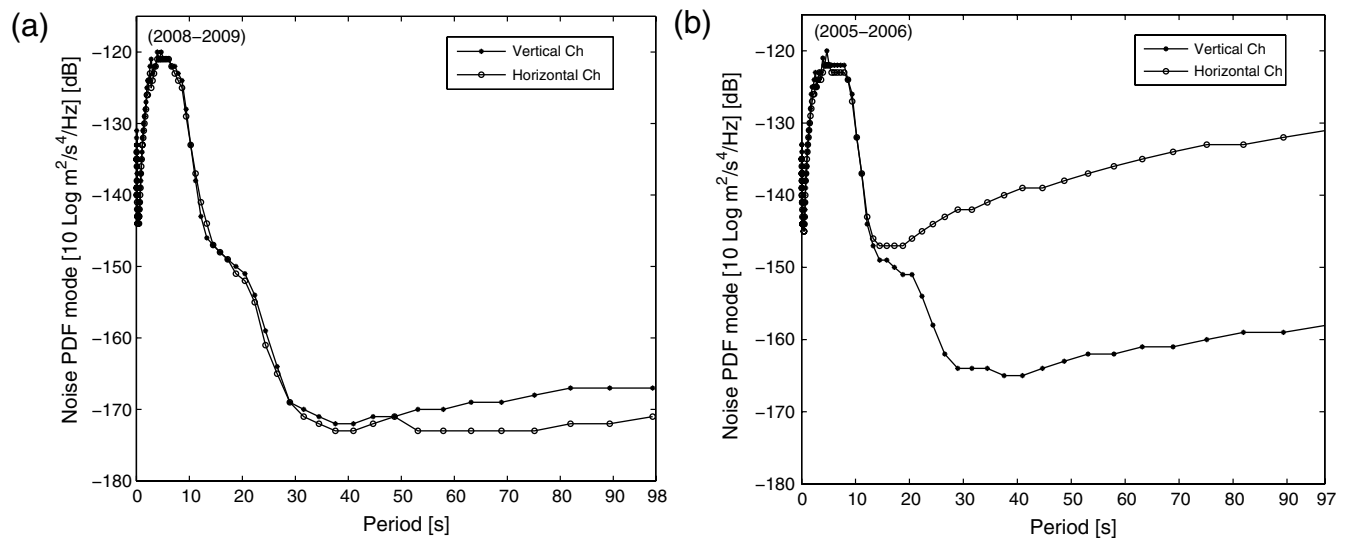


Figure 12. URZ station evaluation for long-period noise: Comparing the vertical and horizontal noise PDF modes for time intervals (a) (2008–2009) and (b) (2005–2006) after and before the occurrence of the split in the noise PDFs plots respectively (see Fig. 3)

obtain an appropriate noise model, the method suggested by McNamara and Buland 2004 was implemented using PQLX software (McNamara and Boaz, 2006; Boaz and McNamara, 2008; McNamara and Boaz, 2011) and applied to the North Island stations' recordings. A stable noise model for each site was then obtained by studying the changes in the stationary parts of the noise models. The available seismic noise sources were then studied and characterized through the noise models. The modes of the corresponding PDFs over all periods were obtained to represent the noise baseline. The noise PDF modes were then compared in different period bands. Studying the noise energy around the period 1.28 s showed that, for the stations located close to the coastlines, the noise levels are 38–55 dB higher than that of the NLNM. However, these differences range from 28 to 34 dB at the TOZ, TLZ, MRZ, BKZ, MWZ, OUZ, TSZ, URZ, and WCZ stations with more distance from the coastlines (see Fig. 1).

The PDF MLNM for the North Island sites was then obtained and shown to be approximately 12–27 dB above the NLNM in the period interval 0.1–1 s. For each station, the maximum and the minimum differences between the North Island MLNM and the corresponding noise PDF mode between 0.1 s and 63.1 s were obtained. The difference levels and their corresponding periods can provide a quick assessment tool (Table 2).

The daily and seasonal changes of the noise PDF modes in different period bands for the stations were then studied. It was in general found that the noise power in the 0.1–1 s period interval was higher from 7 a.m. to 8 p.m. New Zealand local time. The maximum possible variations and their corresponding periods in the cultural band interval during daytime hours were then obtained for each station (Table 3). The PUZ, KUZ, WEL, and TLZ mode noise models were found to show maximum variations in the cultural noise band. This can be either due to their location and/or the installation quality. It was found that MXZ station had the lowest variations over the obtained period interval. Because the MXZ station is located at Matakaoa Point (see Fig. 1) and the short-period noise did not show a large hourly variation, it can be inferred that the noise at periods less than 1 s is mainly caused by the short-period energy due to local wave action. For some stations (URZ, TSZ, OUZ, BKZ, and MRZ), the amount of maximum possible variation dramatically decreased within its corresponding period interval. For the URZ station it can be attributed to the borehole installation of the sensor that can filter the noise energy in periods longer than 0.17 s. For the periods up to 30 s, the noise character generally did not show strong diurnal dependency.

Study of the monthly variations of the noise PDF modes showed that cultural noise power levels increased from October to May (spring–summer) for the TSZ, TOZ, VRZ, URZ, WAZ, WEL, and HIZ stations. Besides, for 70.5% of the stations, the microseism peak value in the 1–4 s band was observed in June, and for 17.5% of the stations the peak was

equally observed in July and August. This is most likely due to the increase in the sea storms during the southern hemisphere winter. In addition, it was shown that the microseism power is enhanced and enriched in short-period energy during the winter time.

Study of the long-period noise variation (longer than 35 s) showed that the noise energy level for the stations KUZ, OUZ, and PUZ increases from late night to morning hours (for example from 12–9 a.m. for the OUZ station). These stations have the same installation design and are relatively close to the sea. Time and dates corresponding to this phenomenon showed that this has mainly occurred during times with lower temperatures. Therefore, it may be due to the convection induced by the seismometer in any open space inside the insulation. These findings suggest an evaluation of the sensor installations at these sites may be beneficial. However, as the KUZ station is located in an old gold mine where temperature variations are expected to be minimal, we cannot make a definitive statement about the cause in this case.

Finally the horizontal and vertical noise PDF modes for the surface vault instruments were compared. The difference in the horizontal and vertical long-period noise can be due to tilt and temperature fluctuations. For the North Island surface vault instruments, the average difference varied from 13 to 33.4 dB. With a proper borehole installation, the difference between the long-period horizontal and vertical noise levels should be small.

In conclusion, this study has shown that the PDF method of McNamara and Buland 2004 and the PQLX software are appropriate techniques for quantifying the ambient noise models for seismograph stations in the North Island of New Zealand.

## Data and Resources

We acknowledge the New Zealand GeoNet project (<http://www.geonet.org.nz>) and its sponsors, the Earthquake Commission of New Zealand (EQC), GNS Science, and Land Information New Zealand (LINZ), for providing seismic data, information on geology, and New Zealand National Seismograph Network (NZNSN) location and sensor history used in this study. The NZNSN seismic data can be downloaded from the GeoNet Earthquake Resources at [www.geonet.org.nz/earthquake/resources](http://www.geonet.org.nz/earthquake/resources). Geonet also provides a facility to search the New Zealand Earthquake Catalogue. The PQLX software package can be downloaded from the software downloads of the IRIS Data Management Center (<http://www.iris.edu/software/downloads>).

The topographic map of the North Island (sourced from Topographic Map 265-1 North Island, Crown Copyright Reserved) can be downloaded from the LINZ website at <http://www.linz.govt.nz/topography/topo-maps/nz-small-scale-maps>. All sites were last accessed in November 2011.

## Acknowledgments

The authors would like to express their appreciation for the kind assistance of Mark Chadwick and Russell Robinson at the GNS (Institute of Geological and Nuclear Sciences, Wellington) and Richard Boaz at Boaz Consultancy (Germany).

This project was funded by Earthquake Commission of New Zealand (EQC).

## References

- Aster, R., D. E. McNamara, and P. Bromirski (2008). Multidecadal climate-induced variability in microseisms, *Seismol. Res. Lett.* **79**, no. 2, 194–202.
- Aster, R. C., D. E. McNamara, and P. D. Bromirski (2010). Global trends in extremal microseism intensity, *Geophys. Res. Lett.* **37**, L14303. doi [10.1029/2010GL043472](https://doi.org/10.1029/2010GL043472).
- Bendat, J. S., and A. G. Piersol (1986). *Random Data: Analysis and Measurement Procedures*, Second Ed., Wiley, New York, 407 pp.
- Berger, J., P. Davis, and G. Ekström (2004). Ambient Earth noise: A survey of the Global Seismographic Network, *J. Geophys. Res.* **109**, no. B11307, doi [10.1029/2004JB003408](https://doi.org/10.1029/2004JB003408).
- Boaz, R. I., and D. E. McNamara (2008). PQLX: A data quality control system: Uses and applications, *Orfeus Newsletter*, **8** no. 1, <http://www.orfeus-eu.org/Organization/Newsletter/vol8no1/PQLX/PQLX.htm> (last accessed November 2011).
- Bormann, P. (2002). Seismic signals and noise, in *New Manual of Seismological Observatory Practice*, P. Bormann (Editor), GeoForschungsZentrum, Potsdam, Germany, 33 pp.
- Bormann, P., K. Wylegalla, and K. Klinge (1997). Analysis of broadband seismic noise at the German Regional Seismic Network and search for improved alternative station sites, *J. Seismol.* **1**, no. 4, 357–381.
- Bromirski, P., and F. Duennebier (2002). The near-coastal microseismspectrum: Spatial and temporal wave climate relationships, *J. Geophys. Res.* **107**, no. B8, doi [10.1029/2001JB000265](https://doi.org/10.1029/2001JB000265).
- Gledhill, K. R. (2004). New Zealand National Seismograph Network, *Report for the Federation of Digital Seismograph Networks Meeting*, Institute of Geological & Nuclear Sciences, Wellington, New Zealand, 9 pp.
- Havskov, J., and J. Alguacil (2004). *Instrumentation in Earthquake Seismology* Springer, Dordrecht, The Netherlands, 358 pp.
- Hedlin, M. A. H., and J. A. Orcutt (1989). A comparative study of island, seafloor and sub-seafloor ambient noise levels, *Bull. Seismol. Soc. Am.* **79**, no. 1, 172–179.
- Holcomb, G., L. Sandoval, and B. Hutt (1998). *Experimental Investigations Regarding The Use Of Sand As An Inhibitor Of Air Convection In Deep Seismic Boreholes*, *U.S. Geol. Surv. Tech. Rept.* 98-362, 56 pp.
- Kurrle, D., and R. Widmer-Schmidrig (2010). Excitation of long-period Rayleigh waves by large storms over the North Atlantic Ocean, *Geophys J Int.* **183**, no. 1, 330–338. doi [10.1111/j.1365-246X.2010.04723.x](https://doi.org/10.1111/j.1365-246X.2010.04723.x).
- McNamara, D. E., and R. I. Boaz (2006). *Seismic Noise Analysis System, Power Spectral Density Probability Density Function: Stand-Alone Software Package*. *U.S. Geol. Surv. Tech. Rept.* 2005-1438, 29 pp.
- McNamara, D. E., and R. I. Boaz (2011). PQLX: A Seismic Data Quality Control System: Description, Applications and Users Manual, *U.S. Geol. Surv. Open-File Report 2010-1292*, 41 pp.
- McNamara, D. E., and R. P. Buland (2004). Ambient noise levels in the continental United States, *Bull. Seismol. Soc. Am.* **94**, no. 4, 1517–1527.
- McNamara, D. E., C. R. Hutt, L. S. Gee, H. M. Benz, and R. P. Buland (2009). A method to establish seismic noise baselines for automated station assessment, *Seismol. Res. Lett.* **80**, no. 4, 628–637.
- Murphy, A. J., and J. R. Savino (1975). A comprehensive study of long-period (20–200 s) Earth noise at the high gain worldwide seismograph stations, *Bull. Seismol. Soc. Am.* **65**, no. 6, 1827–1862.
- Oppenheim, A. V., R. W. Schaffer, and J. R. Buck (1999). *Discrete-Time Signal Processing*, Second Ed., Prentice Hall, Englewood Cliffs, New Jersey, 870 pp.
- Peterson, J. (1993). *Observation And Modeling Of Seismic Background Noise*, *U.S. Geol. Surv. Tech. Rept.* 93-322, 1–95.
- Peterson, J., and J. Orsini (1976). Seismic research observations: Upgrading the worldwide seismic data network. , *Eos, Trans. AGU* **57**, 54.
- Petersen, T., K. Gledhill, M. Chadwick, N. H. Gale, and J. Ristau (2011). The New Zealand National Seismograph Network, *Seismol. Res. Lett.* **82**, no. 1, 9–20.
- Rastin, S. J., C. P. Unsworth, K. R. Gledhill, G. G. Coghill, M. Chadwick, and R. Robinson (2010). PQLX noise model for the URZ station in the Matata Region of New Zealand, *10th International Conference on Information Sciences, Signal Processing and Their Applications (ISSPA)*, 10–13 May 2010, Malaysia, Kuala Lumpur, 17–20, doi [10.1109/ISSPA.2010.5605566](https://doi.org/10.1109/ISSPA.2010.5605566).
- Stensby, J. L. (2011). Random signals and noise, *Course Notes*, <http://www.ece.uah.edu/courses/ee420-500/> (last accessed November 2011).
- Webb, S. C. (2002). Seismic noise on land and the sea floor, in *International Handbook of Earthquake and Engineering Seismology, Part A: International Geophysics*, Vol. **81**, W. H. K. Lee, P. C. Jennings, C. Kisslinger, and H. Kanamori (Editors), Academic Press e-book, 305–318.
- Wielandt, E. (2002). Seismic sensors and their calibration, in *New Manual of Seismological Observatory Practice*. P. Bormann (Editor), GeoForschungsZentrum, Potsdam, Germany, 14 pp.
- Wilson, D. J. Leon, R. Aster, J. Ni, J. Schlue, S. Grand, S. Semken, S. Baldrige, and W. Gao (2002). Broadband seismic background noise at temporary seismic stations observed on a regional scale in the southwestern United States, *Bull. Seismol. Soc. Am.* **92**, no. 8, 3335–3342.
- Withers, M. M., R. C. Aster, C. J. Young, and E. P. Chael (1996). High-frequency analysis of seismic background noise as a function of wind speed and shallow depth, *Bull. Seismol. Soc. Am.* **86**, 1507–1515.

Department of Engineering Science  
University of Auckland  
70 Symonds St., Level 2  
Auckland  
New Zealand  
Private Bag 92019, Auckland 1142  
s.rastin@auckland.ac.nz  
(S.J.R., C.P.U.)

Geological & Nuclear Science  
1 Fairway Drive  
P.O.Box 30-368  
Lower Hutt  
New Zealand  
k.gledhill@gns.cri.nz  
(K.R.G.)

U.S. Geological Survey  
National Earthquake Information Center  
Box 25046, Stop 966  
Denver Federal Center  
Denver, Colorado 80225  
mcnamara@usgs.gov  
(D.E.M.)